Planform Changes in the Lower Mahaweli River, Sri Lanka Using Landsat Satellite Data

land

MDPI

Article

Planform Changes in the Lower Mahaweli River, Sri Lanka Using Landsat Satellite Data

Vindhya Basnayaka [1], Jayanga T. Samarasinghe [2], Miyuru B. Gunathilake [3,4], Nitin Muttil [5,6] and Upaka Rathnayake [1,*]

[1] Department of Civil Engineering, Faculty of Engineering, Sri Lanka Institute of Information Technology, Malabe 10115, Sri Lanka
[2] Department of Earth Environmental and Resource Sciences, University of Texas, El Paso, TX 79968, USA
[3] Hydrology and Aquatic Environment, Environment and Natural Resources, Norwegian Institute of Bioeconomy and Research, 1433 Ås, Norway
[4] Water, Energy and Environmental Engineering Research Unit, Faculty of Technology, University of Oulu, P.O. Box 8000, FI-90014 Oulu, Finland
[5] Institute for Sustainable Industries & Liveable Cities, Victoria University, P.O. Box 14428, Melbourne, VIC 8001, Australia
[6] College of Engineering and Science, Victoria University, Melbourne, VIC 8001, Australia
* Correspondence: upaka.r@sliit.lk or upakasanjeewa@gmail.com

Abstract: Major development projects along rivers, like reservoirs and other hydraulic structures, have changed not only river discharges but also sediment transport. Thus, changes in river planforms can be observed in such rivers. In addition, river centerline migrations can be witnessed. The Mahaweli River is the longest in Sri Lanka, having the largest catchment area among the 103 major river basins in the country. The river has been subjected to many development projects over the last 50 years, causing significant changes in the river discharge and sediment transport. However, no research has been carried out to evaluate the temporal and spatial changes in planforms. The current seeks to qualitatively analyze the river planform changes of the Lower Mahaweli River (downstream to Damanewewa) over the past 30 years (from 1991 to 2021) and identify the major planform features and their spatiotemporal changes in the lower Mahaweli River. Analyzing the changes in rivers requires long-term data with high spatial resolution. Therefore, in this research, remotely sensed Landsat satellite data were used to analyze the planform changes of Lower Mahaweli River with a considerably high resolution (30 m). These Landsat satellite images were processed and analyzed using the QGIS mapping tool and a semi-automated digitizing tool. The results show that major changes in river Mahaweli occurred mainly in the most downstream sections of the selected river segment. Further, the river curvature was also comparatively high downstream of the river. An oxbow lake formation was observed over time in the most downstream part of the Mahaweli River after 2011. Centerline migration rates were also calculated with the generated river centerlines. It was found that the rates were generally lower than about 30 m per year, except for at locations where river meandering was observed. The main limitations of this study were the possible misclassifications due to the resolution of images and obstructions caused by cloud cover in the Landsat images. To achieve more accurate estimates, this study could be developed further with quantitative mathematical analysis by also considering the sediment dynamics of the Mahaweli River.

Keywords: river morphodynamics; centerline migration; Landsat data; planform changes; remote sensing

Citation: Basnayaka, V.; Samarasinghe, J.T.; Gunathilake, M.B.; Muttil, N.; Rathnayake, U. Planform Changes in the Lower Mahaweli River, Sri Lanka Using Landsat Satellite Data. *Land* **2022**, *11*, 1716. https://doi.org/10.3390/land11101716

Academic Editors: Matej Vojtek, Andrea Petroselli and Raffaele Pelorosso

Received: 11 September 2022
Accepted: 30 September 2022
Published: 3 October 2022

1. Introduction

The geomorphology of rivers is highly dynamic and has to be closely monitored. Most of the large meandering rivers in the world, which carry significant sediment loads, are subjected to change over time [1]. In fact, braided rivers exhibit high variability within

short periods [2]. These changes are often due to sediment movement, river hydraulic and hydrological processes, topography, and the vegetation properties of the riverine environments [3]. Studying the geomorphological changes in rivers is paramount in understanding the natural dynamics and will be helpful in predicting the patterns of future planform changes [4]. The knowledge gained through these analyses will be significant in the decision-making stage of river and floodplain management.

According to the literature, many investigations have been carried out for in recent decades on river planform changes, although these analyses represent different scales and have adopted different methods [3–8]. In many historical studies (during the 1990s and early-2000s), researchers used field data, analytical models, or numerical models to analyze river planform dynamics [9–12]. With the massive development of technology in recent years, more sophisticated computers with high computing power and satellite remote sensing data have become available. Therefore, most recent studies have taken advantage of remotely sensed satellite data (geospatial imagery) and tools such as GIS and algorithms, developed with programming languages such as MATLAB and Python [12]. In some cases, the spatial scale of river planform changes were only a few meters, while in others, there were migrations of up to a few hundred meters. Hence, the need arises for data with high spatial and temporal resolution [13]. Further, this will be crucial when analyzing highly dynamic rivers that contain large numbers of meandering bends.

To analyze the planform changes in rivers, long-term records of the river geomorphology are required. However, in many countries, there are no such databases that contain constant and long-term records of river planforms. This limitation is addressed by using remotely sensed data [14]. With the recent advancements in technology, the availability of free data has been hugely increased. Therefore, these remotely sensed data are used in many projects and research, not only in the water sector but also in many other fields. The importance of remotely sensed satellite data are their free and global availability and considerably high resolution (about 30 m). Further, some of these data are available for more than 30 years (ex: Landsat satellite data is available since 1984) [15].

Many researchers all over the world have used Landsat data to investigate the temporal variation of river meandering [16]. As it was stated, these techniques are chosen ahead of onsite surveying due to logistic and financial issues. Wray [17] has used multispectral Landsat imagery to observe the changes in Palaeochannels of the Namoi River, New South Wales, Australia. Landsat 7 ETM+ data were used in this analysis and the historical changes in Namoi River were presented. Schwenk et al. [18] have incorporated the RivMAP toolbox with Landsat images to detect the physics in meandering migrations in multi-decades for the Ucayali River (which is the headstream of the Amazon River). Therefore, the usage of Landsat data by linking them to the analyzer revealed the significance of such data for the evaluation of river meandering. In addition, Nagel et al. [19] used cloud computing with Landsat data to understand the migration of communities along the Amazon River due to the meandering course of the river. Therefore, the indirect impacts were also assessed based on Landsat data.

However, other than by Basnayaka et al. [15], these recent advances have not been applied in Sri Lanka to understand the meandering behavior of rivers. The River Mahaweli is important due to its flat bathymetry downstream. In addition, the sediment flow is obstructed by several reservoirs along the river. Therefore, assessments of the temporal variation of the river, in terms of its meandering and planform changes, are essential. However, survey data along the river section are limited. Thus, this research addresses these research gaps by analyzing Landsat images of the Mahaweli River to identify the major planform features and their spatial and temporal variation over a 30 year period from 1991 to 2021. The findings of this research will be helpful for managing the riverine environment of the Lower Mahaweli River. Additionally, the proposed method is also applicable for narrow rivers (widths of less than 100 m and greater than the spatial resolution of the imagery, i.e., 30 m) as the method considers only river centerline variations.

2. Study Area and Problem Statement

Among the 103 major river basins in Sri Lanka, Mahaweli is the largest river basin with a catchment area of about 10,448 km^2 [20], which is nearly one-sixth of the country. Further, the Mahaweli River is the longest in Sri Lanka, with a length of about 335 km. The annual precipitation received by the whole basin amounts to 28 $\times$ 10^9 m^3 and the river has an annual discharge of 8.8 $\times$ 10^9 m^3 [20]. According to the Köppen-Geiger climate classification [21], the upper Mahaweli basin belongs to the equatorial fully humid climate zone, while the lower Mahaweli basin lies in the equatorial monsoonal climate zone. River Mahaweli has been subjected to many development projects including hydropower generation projects, supplying drinking water, and agriculture development projects since the beginning of the 1970s. The river has been subjected to many pieces of research which are mostly related to water quality, hydro-meteorological characteristics, sediments geochemistry, water demand management, etc. [22–24]. However, the river morphodynamics of the Mahaweli River is a subject that still needs attention.

Figure 1 clearly showcases the complex river paths of the Mahaweli River (refer to Figure 1a,c) and its meandering behavior of Mahaweli River (refer to Figure 1b). In addition, the river planforms are highly observable (refer to Figure 1c) and they are dynamic based on the flow characteristics depending on the monsoons. Therefore, these observations re-state the importance of having a scientific analysis of the temporal variation of meandering behavior and the river planforms. Thus, a segment of the Mahaweli River to perform the analysis of planform variation over time was selected in this study. The selected river segment is the lower Mahaweli River starting from Damanewewa up to the sea outfall in Trincomalee and has a total length of about 107 km (around 1/3 of the river). The selected river segment is illustrated in Figure 2. The red color box shows the region of interest (ROI) which is Lower Mahaweli River from Damanewewa to Trincomalee.

(**a**)

(**b**)

(**c**)

Figure 1. River meandering behavior: (**a**) Mahaweli River near its sea outfall; (**b**) sediment deposition along the river; (**c**) complex river path with river planforms (source: Google maps).

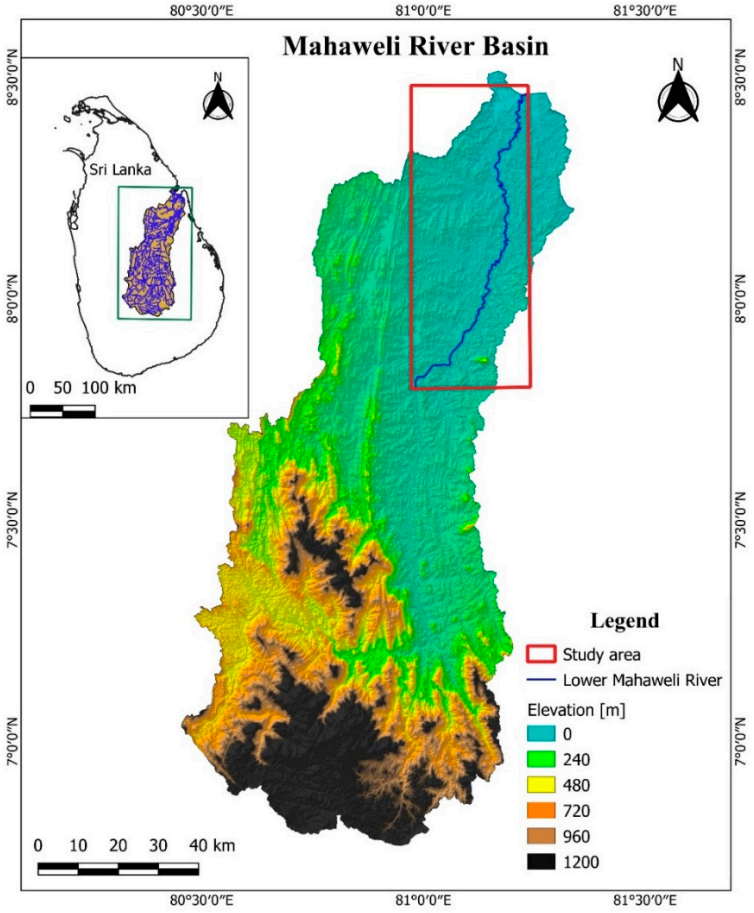

Figure 2. Map of the Mahaweli River basin, Sri Lanka and the selected river segment for the analysis.

3. Data and Methods

3.1. Use of Landsat Imagery

Landsat satellite images provide the most comprehensive record (more than 35 years) for medium resolution (10–50 m) global scale Earth Observation data [25]; images are captured at approximately 16 day intervals. The Landsat mission started in 1984 and continues to today. Currently, there are four Landsat products: Landsat 1–5 MSS, Landsat 4–5 TM, Landsat 7, and Landsat 8–9. The application of Landsat data is widespread because of their free and global scale availability for a considerably long period (about 35 years). Yet, one major issue of these data is obstructions caused by the clouds. Further, in some of the L7 images, there are missing data stripes due to a failure that occurred in the scan line corrector (SLC) [18]. Therefore, in our study, these data were exempted in selecting the imagery. The current study uses only two types of Landsat data, i.e., Landsat 4–5 Thematic Mapper (TM), and Landsat 8 Operational Land Imager (OLI) and Thermal Infrared Sensors (TIRS) products, to estimate the spatiotemporal variability of river planform of Mahaweli River.

There are several methods to download or access Landsat data, including the United States Geological Survey (USGS) website, other environmental data catalogues such as USGS EarthExplorer, LandsatLook Viewer, USGS GloVis, and data catalogues available in cloud-based platforms like Google Earth Engine [26]. To analyze the river planform changes in the Mahaweli River, we downloaded Landsat images from the USGS Earthexplorer website for 30 years spanning from 1991 to 2021. To have a more accurate classification, Landsat images were selected based on the cloud cover criterion. Images with the least cloud cover on the river were selected by visually inspecting the available images. Since the selected three river segments are distributed over two Landsat tiles, (path -141, row–54, 55; refer to Figure 3) both tiles were downloaded and merged using version 3.16 of QGIS

software. A tile has 5000 × 5000 pixels with a resolution of 30 m. Before starting the image classification, all the data were cropped to the interested area to reduce the processing time.

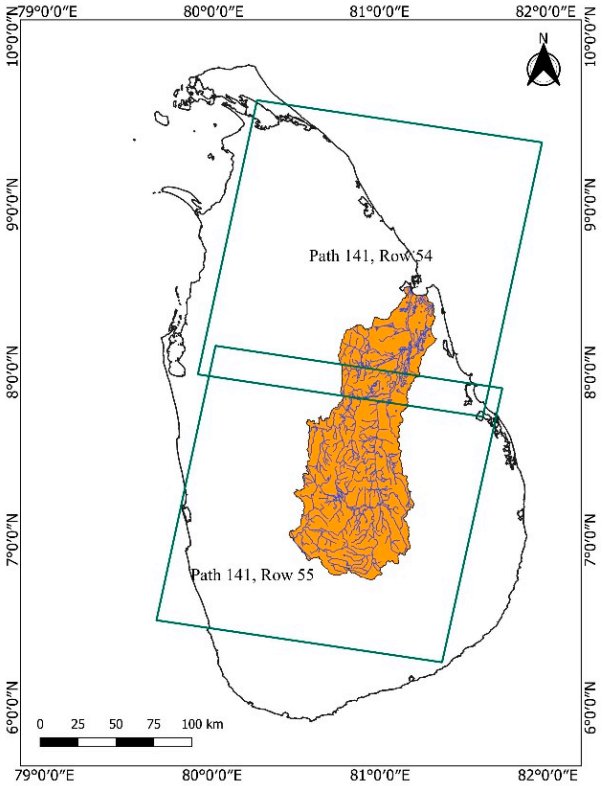

Figure 3. Arrangement of Landsat scenes covering the study area.

3.2. Generating the River Masks

The first step in evaluating the planform changes in the Mahaweli River was to extract the river masks for each selected year using Landsat imagery. Different techniques are used in the literature [27–34] to extract surface water pixels from Landsat images. Index-based classification is one such method that is used to identify water pixels in satellite remote sensing data. Commonly used water indexes are Automated Water Extraction Index for images with shadows ($AWEI_{shadow}$) [27], Tasselled Cap Wetness (TCW_{Crist}) index [28], Normalized Difference Water Index (NDWI) [29], Modified Normalized Difference Water Index (MNDWI) [30], and Automated Water Extraction Index for images without shadows ($AWEI_{no\ shadow}$) [31], Water Index (WI_{2006}) [32], Water Index (WI_{2015}) [33] and Water Index (WI_{2018}) [34].

In the current study, first, we used three water indices to generate the water masks from Landsat images, considering the accuracy of each index in classifying the water pixels. According to Fisher et al. [31], the accuracy of classifying water pixels has slightly increased in WI_{2015} compared to the WI_{2006}. The water index introduced by Raheem and Alwan (WI_{2018}) [34] outperforms most of the previously defined water indices in the classification of water pixels and is comparable to the MNDWI. The mathematical expressions for these indices are given in literature and these are presented in Table 1.

Table 1. Different water indexes defined in literature for water pixel classification using multi-spectral Landsat satellite data. (Surface reflectance values (ρ) of the seven bands are indicated as $\rho_{B1} - \rho_{B7}$ and are the inputs for the equations).

Index	Equation	Source
NDWI	$\frac{\rho_{B2} - \rho_{B4}}{\rho_{B2} + \rho_{B4}}$	[29]
MNDWI	$\frac{\rho_{B2} - \rho_{B5}}{\rho_{B2} + \rho_{B5}}$	[30]
TCW_{Crist}	$0.0315\rho_{B1} + 0.2021\rho_{B2} + 0.3102\rho_{B3} + 0.1594\ \rho_{B4} - 0.6806\rho_{B5} - 0.6109\rho_{B7}$	[28]
$AWEI_{shadow}$	$\rho_{B1} + 2.5 \times \rho_{B2} - 1.5 \times (\rho_{B4} + \rho_{B5}) - 0.25 \times \rho_{B7}$	[27]
$AWEI_{no\ shadow}$	$4 \times (\rho_{B2} - \rho_{B5}) - (0.25 \times \rho_{B4} + 2.75 \times \rho_{B5})$	[30]
WI_{2015}	$1.7204 + 171\rho_{B2} + 3\rho_{B3} - 70\rho_{B4} - 45\rho_{B5} - 71\rho_{B7}$	[33]
WI_{2018}	$\frac{0.12\rho_{B1} + 0.231\rho_{B4}}{0.752\rho_{B6} + 0.223\rho_{B5}}$	[34]

However, the use of these indices alone did not allow us to accurately classify surface water. One major reason for these classification errors may be the presence of mixed water areas such as wetlands. Therefore, it was decided to use Modified Normalized Difference Water Index (MNDWI) together with two vegetation indices; Normalized Difference Vegetation Index (NDVI) and Enhanced Vegetation Index (EVI), as suggested in the literature [35–38] to reduce the misclassification of water areas. The NDVI is used to identify the vegetation percentages by accounting for the greenness of each pixel, while EVI has the capability to correct the atmospheric disturbances and noise from canopy backgrounds [39]. The relationship of MNDWI > NDVI and MNDWI > EVI was used to find out the pixels where the water signals are greater than the vegetation signals and to remove the effect of mixed water and vegetation. The thresholds of EVI were selected following a trial-and-error method by comparing the water masks with Google Earth images. The reflectance values of the images can be affected by the atmospheric condition that exists at the time of acquiring the images. Therefore, the use of different thresholds for different images can be justifiable considering the above fact. These resulting raster images were then used in delineating the river centerlines with the use of the WebPlotDigitizer tool [40].

3.3. Cleaning the River Masks

Having a well-defined river centerline is necessary for the estimation of river direction, curvature, and migration rates and patterns. Therefore, the created watermasks were cleaned before digitizing the centerline to remove the misclassified pixels and have a continuous connection to the river. Further, it removes the unwanted areas such as the water pixels that are not hydraulically connected to the main river (i.e., tributaries, remainders of cut-off channels, and riverside cities).

3.4. Delineating River Centerlines

WebPlotDigitizer is a semi-automated digitizing tool that can be used to automatically digitize images, plots, or maps. In the current study, version 4.5 of WebPlotDigitizer was used [40] to delineate the centerline of the river using the binary watermask. As the first step, images of watermask map were loaded into the WebPlotDigitizer. Then the image was georeferenced using four known points (two points on the X axis and two points on the Y axis). WebPlotDigitizer software allows users to select the method of digitizing; either to digitize the plots/images automatically or manually. When digitizing, the software creates points along the river within a user-specified distance. To have a continuous connection to the river, the gaps of channel masks need to be filled manually by adding additional points for the centerline. The coordinates of these points can be then saved as a comma-separated values (.csv) file or directly copy the data to an Excel or a text file. When saving the (X, Y) coordinate data were arranged in the order from upstream to downstream.

3.5. Estimation of River Planform Geometry

Three parameters were calculated to identify the spatial and temporal variations of the river centerline in the Mahaweli River. The distance between two points of the river

centerline (ds_i), inflection angle (θ_i) and the curvature (c_i) between two successive points (x_i, y_i) and (x_{i+1}, y_{i+1}) along the centreline was computed by the Equations (1)–(3).

$$ds_i = \sqrt{(x_{i+1} - x_i)^2 + (y_{i+1} - y_i)^2} \quad (1)$$

$$\theta_i = arctan(\frac{y_{i+1} - y_i}{x_{i+1} - x_i}) \quad (2)$$

$$c_i = \frac{\theta_{i+1} - \theta_{i-1}}{ds_{i+1} - ds_{i-1}} \quad (3)$$

The two parameters, i.e., inflection angle and curvature, can be used to identify the bends of a river. The zero crossing points of the curvature represent meandering bends [8]. Therefore, the above three parameters were calculated and plotted to study the spatial variation of the Mahaweli River from upstream to downstream. A schematic diagram that illustrates the relationship between curvature and inflection points are shown in Figure 4. The points 1–8 represent the inflection points where the bends are separating.

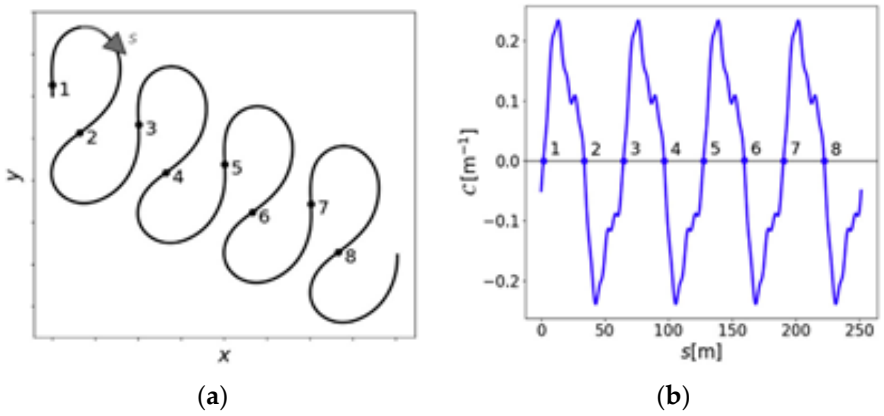

(**a**) (**b**)

Figure 4. Schematic diagram of bend separation using curvature of the channel: (**a**) Bends; (**b**) inflection points [8].

3.6. Calculating the Centerline Migration

The centerline coordinates extracted from the WebPlotDigitizer tool were used to map the river centerlines for the selected nine years. These point data were loaded into the QGIS software to create the polylines for centerlines. Then the geometric attribute tools of QGIS were utilized in calculating the centerline migration between two adjacent years. The centerline migration distances were calculated with an interval of 200 m along the centerline, with the help of geometric attribute tools in QGIS. To compute the migration rates, these migrated distances were then divided by the number of years between the considered two scenarios and obtained the annual migration rates.

3.7. Overall Methodology

The overall methodology carried out in this research is summarized in Figure 5. The extracted Landsat images spanning from 1991 to 2021 were processed as shown in the following flow chart to understand the temporal variation of river planforms in the lower Mahaweli River.

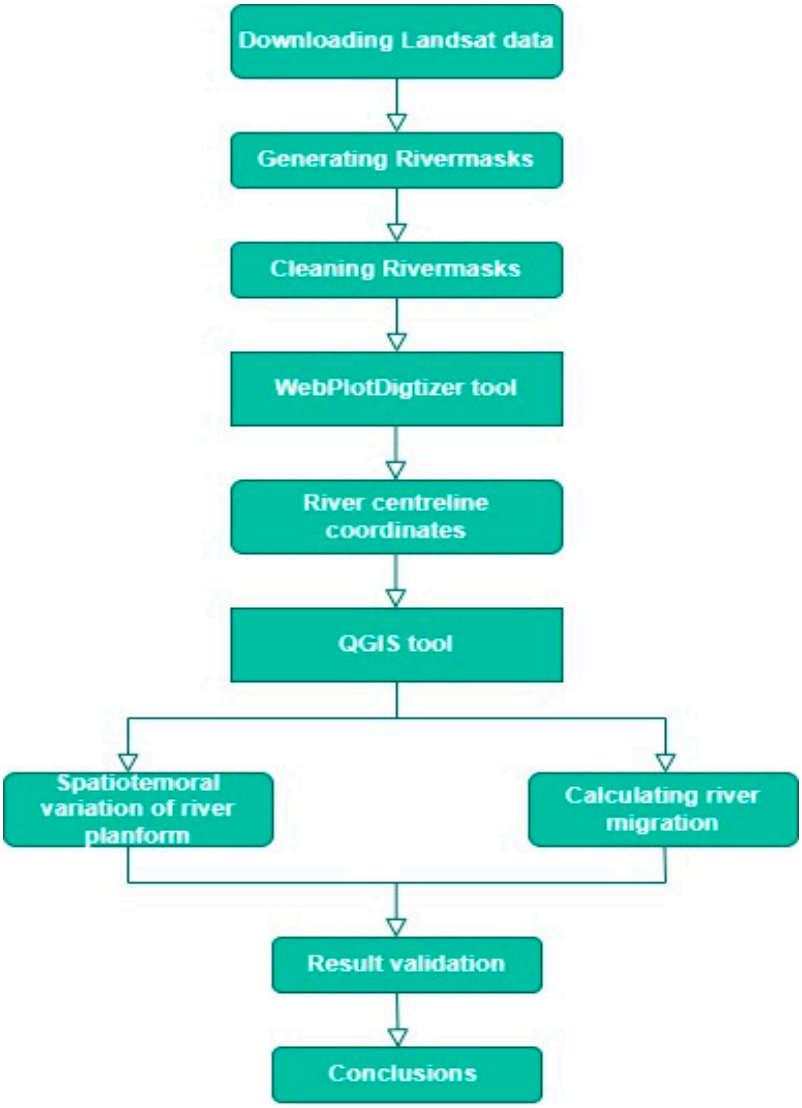

Figure 5. Flowchart of the overall methodology of the study.

4. Results and Discussion

4.1. River Planform

The annual river masks of the Mahaweli River were analyzed to quantify the planform variations from 1991 up to 2021. As the selected river stretch has a total length of 107 km, it was divided into four sections. The generated river masks are presented in Figure 6. Considering the availability of cloud-free images and the selected time span, nine years were selected for our analysis.

It can be seen from river masks that there are disconnections in the main river in a few places. These can occur due to the misclassifications of pixels. These disconnections are indicated in red color boxes (refer to Figure 6b). One of the major reasons for these errors is the cloud cover in the selected images. Additionally, errors can be attributed to the lowered resolution of images compared with the river width. Sometimes, the Landsat images may not be able to capture the river in narrow areas, i.e., where the width of the river is smaller or close to the pixel size (30 m). The river braiding/anabranching areas are highlighted in yellow. Along the selected river segment of the Mahaweli River, there were four clearly visible braided areas, as marked in Figure 6. According to the extracted river masks, an oxbow lake formed near Trincomalee at the most downstream point of the Mahaweli River. This lake formation is illustrated in Figure 6a with a green box.

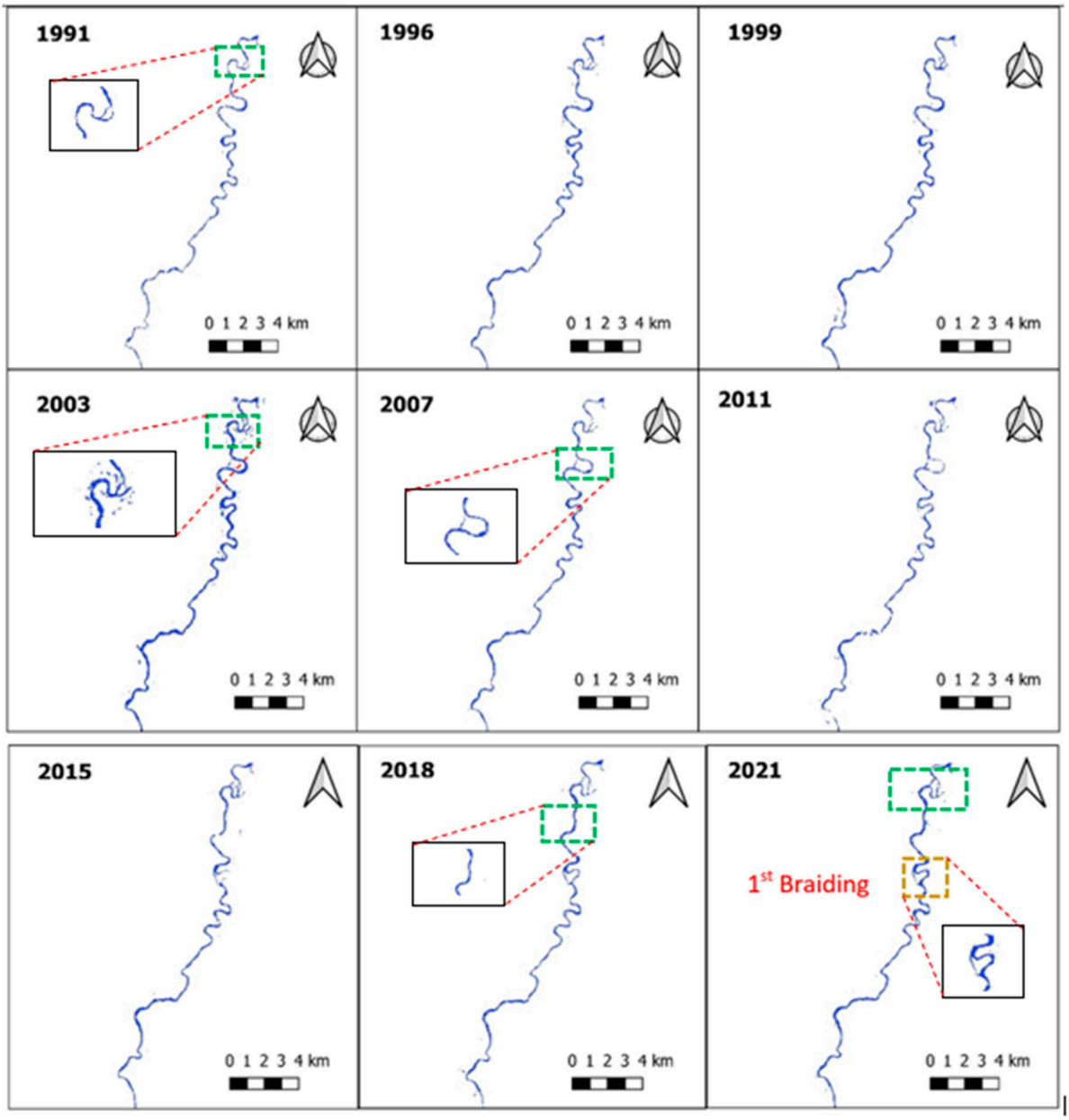

(**a**)

Figure 6. *Cont*.

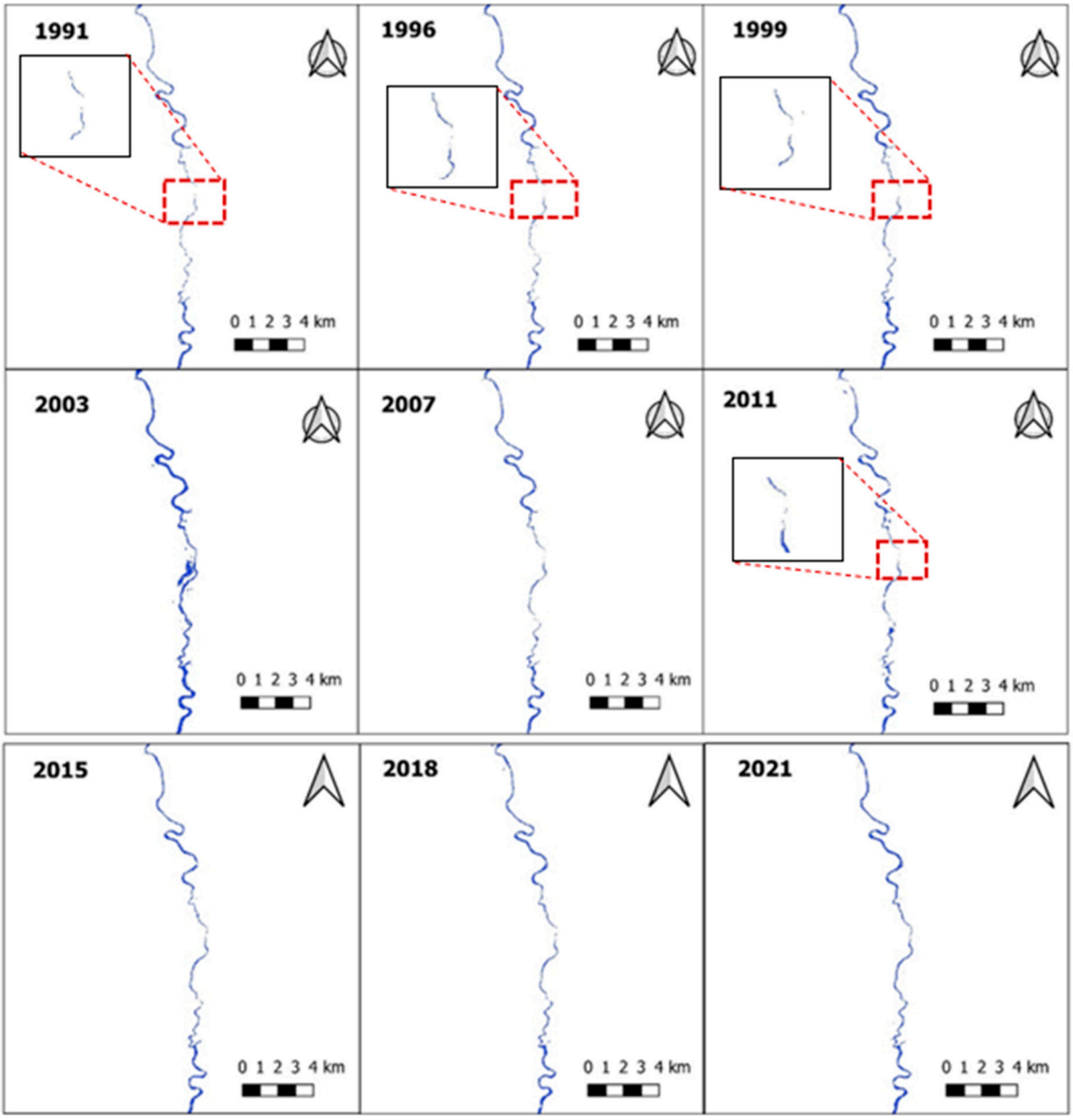

(**b**)

Figure 6. *Cont*.

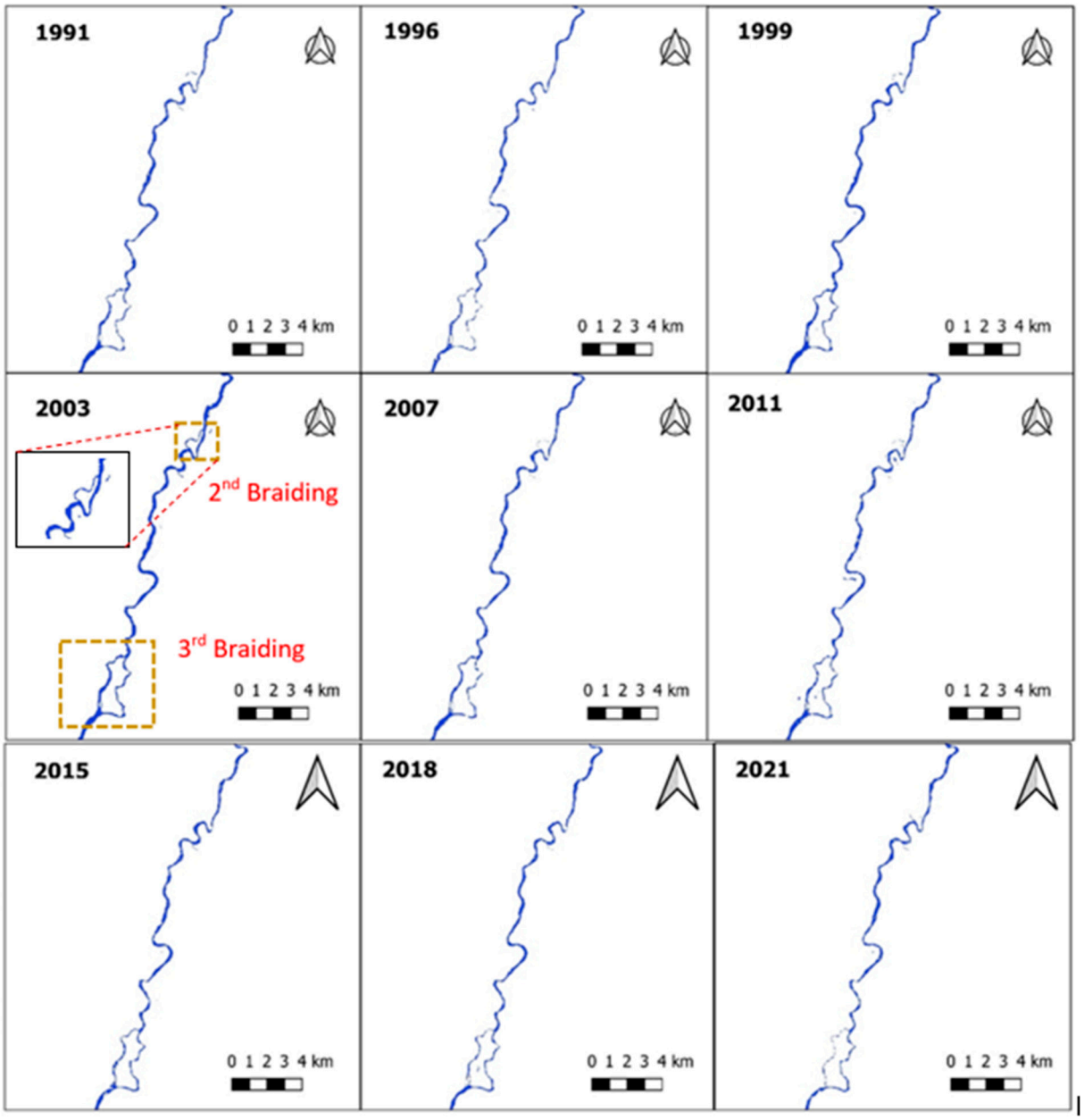

(**c**)

Figure 6. *Cont*.

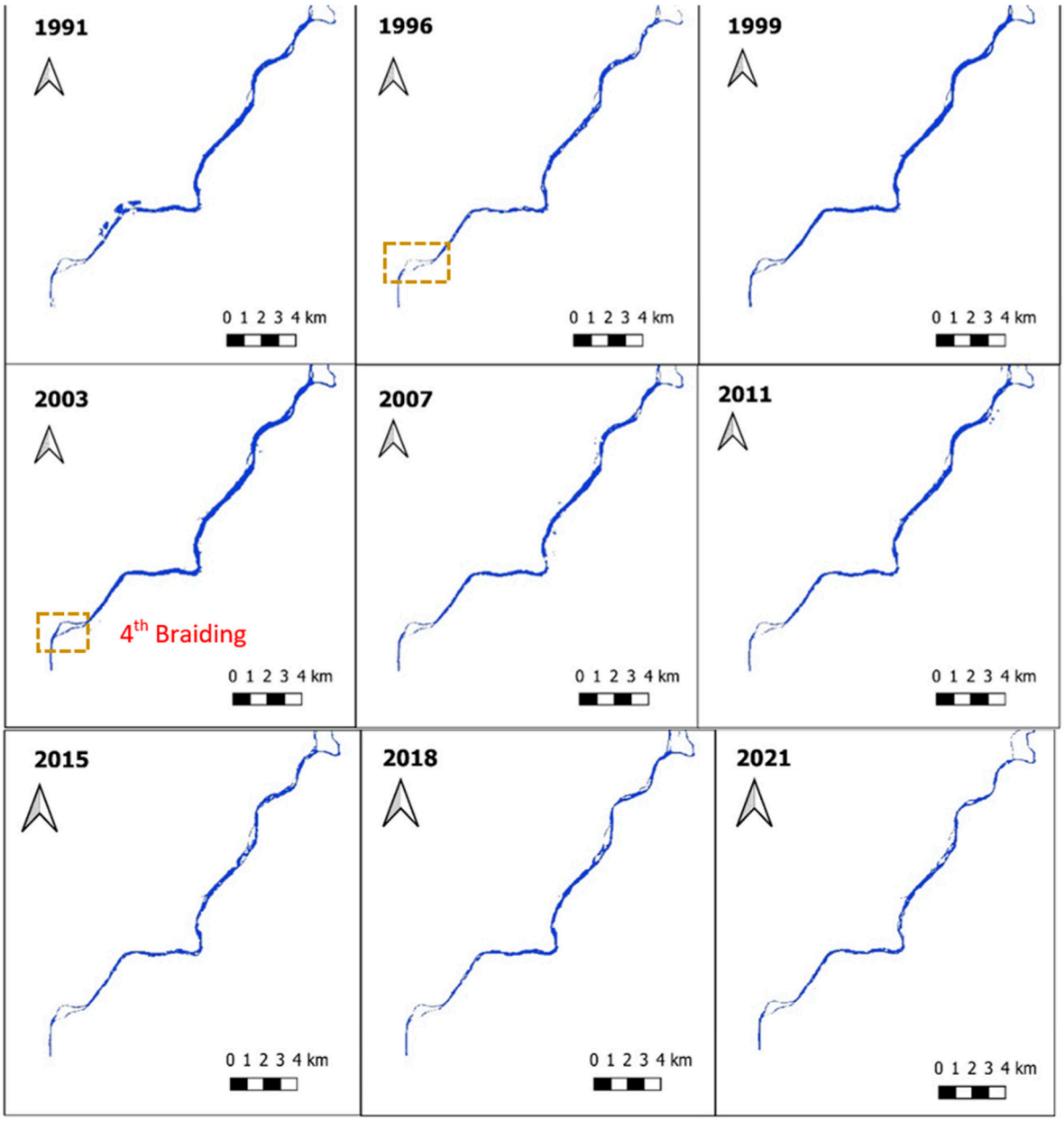

(**d**)

Figure 6. River masks generated for the Mahaweli River from Damanewewa to Trincomalee: (**a**) Most downstream river part of the selected Mahaweli River stretch near to Trincomalee; (**b**,**c**) middle stretches of the selected river segment; (**d**) most upstream part of the selected river stretch starts from Damanewewa.

4.2. Spatiotemporal Variation of River Centreline

The river centerlines points extracted from the watermasks were processed in QGIS to create the centerlines and compare the variations. The centerlines of the main river are presented in Figure 6. Since centerline migrations in the considered river stretch were mainly observed at the most downstream sections of Mahaweli River, here we have presented only the stretch (a) described in the previous sub-section. The figure shows the formation of an oxbow lake (highlighted in red color) over time during these 30 years. The location of the oxbow lake observed downstream of the Mahaweli River is highlighted in Figure 7.

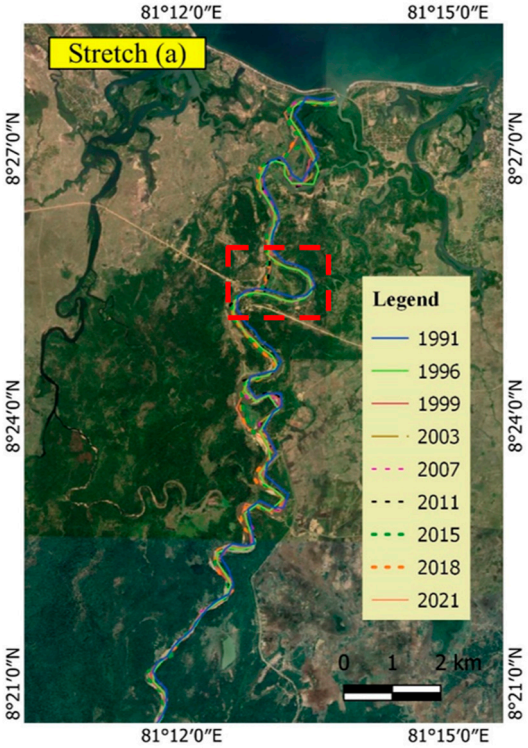

Figure 7. Temporal variation of river centerline.

4.3. Variation of River Curvature

The river curvature for each year was computed and plotted against the distance along the river centerline. These high curvatures represent the locations of bends along the river. As shown in Figure 8, the frequency of high curvature bends increases in the downstream direction. The high curvature of rivers drives the meandering process by causing erosion in the outer bank and accretion in the inner bank. The river curvature values are comparable with the values obtained in a similar study done for Deduru Oya in Sri Lanka [15]. However, the maximum curvature of the selected segment of the Mahaweli River is higher than that of the Deduru Oya River. According to the literature [41], the average bend curvature is related to the average migration rate of a certain river bend. Therefore, these river curvature values are indications of possible meandering bends in the selected river segment.

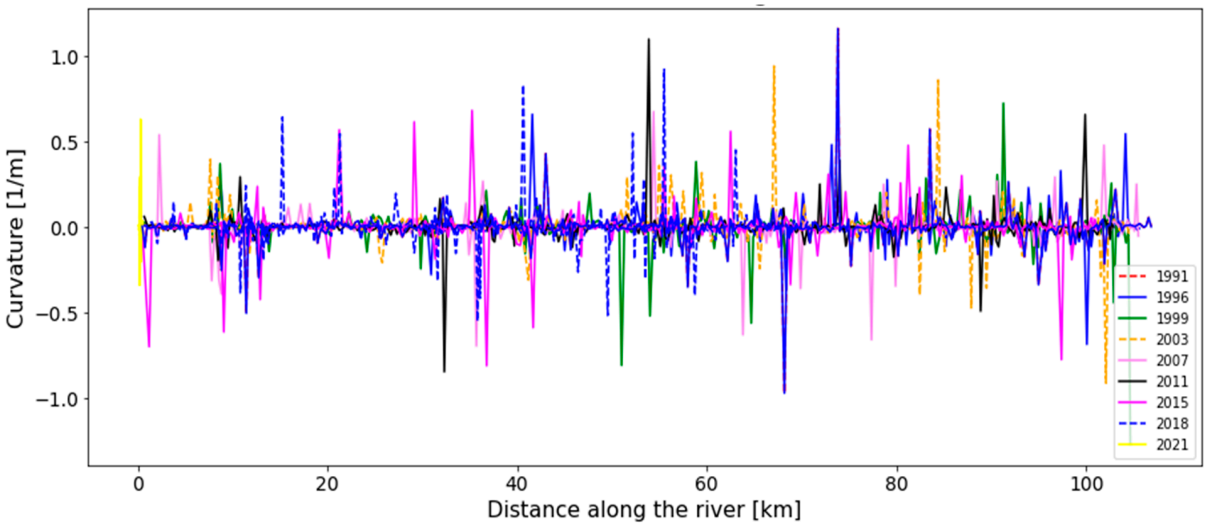

Figure 8. Spatial and temporal variation of river curvature.

4.4. Variation of River Centreline Migration

To estimate the evolution of the river, centerline migration rates were computed as described in Section 3.6. The migration rates were plotted against the distance along the river centerline and are illustrated in Figure 9. The results show three major spikes in the annual migration rates during the periods 2011 to 2015 and 2015 to 2018. This can be attributed to the changes in the main river flow path that occurred with the oxbow lake formations (during 2007 and 2011) and sediment bar formations. To have a clearer estimate of these changes, a mathematical analysis needs to be carried out including the data about riverbanks and sediment bars. The spatial variation of the annual migration rates shows that the upstream areas of the selected river segment have fewer rates of centerline migrations than the downstream segments. This can be explained considering the meandering of the high curvature bend in the river (mainly the downstream of Mahaweli River).

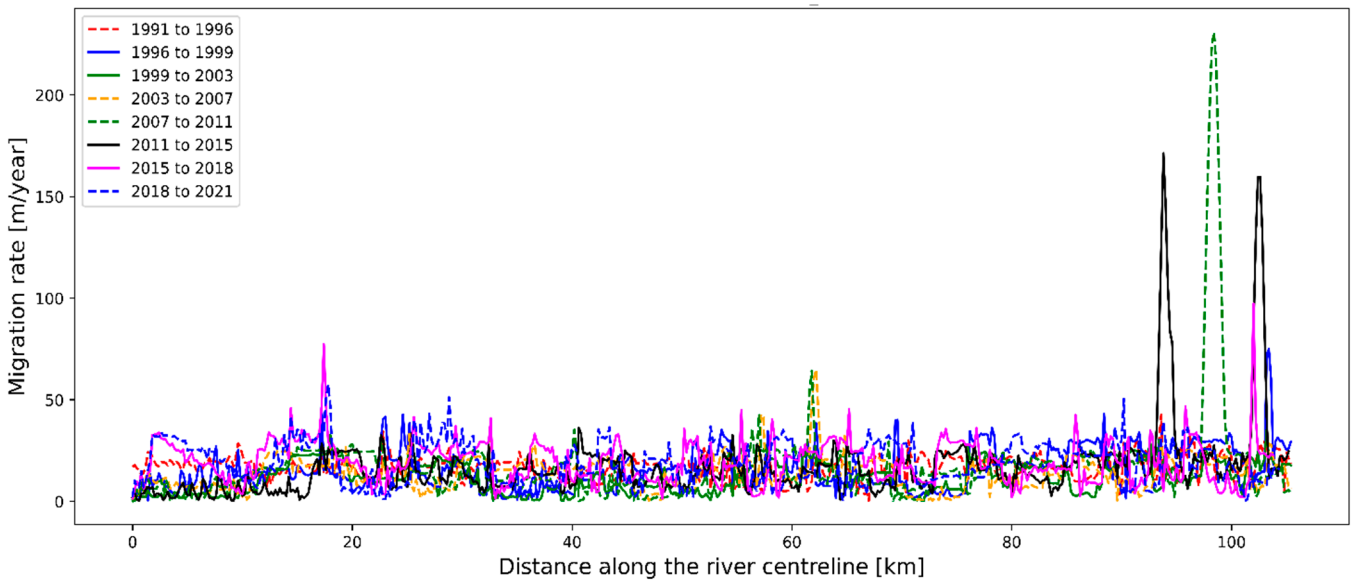

Figure 9. Spatial and temporal variation of river centerline migration rates.

When compared with the river migration rates of Deduru Oya, the Lower Mahaweli River exhibits minor values except for the three bends described above. The average centerline migration rates are within the limit 20–40 m/year.

5. Summary and Conclusions

This study focused on the longest river in Sri Lanka, whose catchment are accounts for approximately one-sixth of the country's territory. Landsat satellite images were used to identify the major planform changes over thirty years from 1991 to 2021, in Lower Mahaweli River, exhibiting the dynamic nature in its geomorphology. In the selected river segment, there were four locations where river braiding could be clearly observed. During the past three decades, there were no considerable changes in the planform of the Lower Mahaweli River, although small seasonal migrations could be seen in the upstream parts. However, the downstream segments of the river exhibited significant changes over time. With the extracted watermasks, the creation of an oxbow lake near Trincomalee was identified. The migration rates were calculated for the river centerlines; it was found that the rates were generally lower than about 30 m per annum. There were three locations where the annual migrations were more than 100 m; these may be the locations where the main flow path changed due to oxbow lake formation and sediment bar depositions. The overall results of this study highlight the need for quantitative analyses, especially in the downstream areas of the Lower Mahaweli River.

The accuracy of these geospatial analyses depends strongly on the resolution of the images. Medium resolution satellite images are a good source of data for analyzing the planform changes of a river when there are no or limited field data available. However, cloud coverage in these satellite images is a major limitation. Therefore, using satellite images that are not impeded by clouds or a lack of illumination is suggested. However, currently, such satellite data are not freely available for long-term analyses, as the images obtained with active sensors (Sentinel 1) like synthetic aperture radar (SAR) are only available for very short periods (Sentinel 1 is available only after 2014).

In the current research, the major features of the Mahaweli River planform and their temporal and spatial variations were identified. However, the methodology was designed only for a qualitative analysis as an initial study, because, to the best of the authors' knowledge, no such research has analyzed the river planform geomorphology and its variations over such a long period using remote sensing technology. The current study is therefore an introductory work for future detailed mathematical analyses.

The methodology proposed in the current study is applicable to a vast range of river planform studies, mainly for rivers which are narrower than 100 m. Nevertheless, the results of our qualitative analysis could be used to manage water resources in the downstream of the Mahaweli River. The area near the sea outlet of the Mahaweli River is interesting, as it has one of the world's most famous natural harbors.

Author Contributions: Conceptualization, U.R.; methodology, V.B. and J.T.S.; software, V.B., J.T.S. and M.B.G.; formal analysis, V.B. and J.T.S.; resources, V.B. and M.B.G.; data curation, V.B. and J.T.S.; writing—original draft preparation, V.B. and J.T.S.; writing—review and editing, U.R. and N.M.; visualization, V.B. and J.T.S.; supervision, U.R.; project administration, U.R. All authors have read and agreed to the published version of the manuscript.

Funding: This research received no external funding.

Data Availability Statement: The data presented in this research work can be obtained from the corresponding authors for research purposes.

Conflicts of Interest: The authors declare no conflict of interest.

References

1. Constantine, J.A.; Dunne, T.; Ahmed, J.; Legleiter, C.; Lazarus, E. Sediment supply as a driver of river meandering and floodplain evolution in the Amazon Basin. *Nat. Geosci.* **2014**, *7*, 899–903. [CrossRef]
2. Zanoni, L.; Gurnell, A.; Drake, N.; Surian, N. Island dynamics in a braided river from analysis of historical maps and air photographs. *River Res. Appl.* **2008**, *24*, 1141–1159. [CrossRef]
3. James, J.S.H.; Rogala, T.; Fitzpatrick, F.A. Recent Planform Changes in the Upper Mississippi River. U.S. Geological Survey. Upper Midwest Environmental Sciences Center. 2020. Available online: https://www.usgs.gov/publications/recent-planform-changes-upper-mississippi-river (accessed on 1 September 2022).
4. Rădoane, M.; Perşoiu, I.; Cristea, I.; Chiriloaei, F. River channel planform changes based on succesive cartographic data. A methodological approach. *J. Geomorphol.* **2013**, *15*, 69–88.
5. Monegaglia, F.; Zolezzi, G.; Güneralp, I.; Henshaw, A.J.; Tubino, M. Automated extraction of meandering river morphodynamics from multitemporal remotely sensed data. *Environ. Model. Softw.* **2018**, *105*, 171–186. [CrossRef]
6. Deb, M.; Das, D.; Uddin, M. Evaluation of Meandering Characteristics Using RS & GIS of Manu River. *J. Water Resour. Prot.* **2012**, *4*, 163–171. [CrossRef]
7. Dey, A.; Bhattacharya, R.K. Monitoring of River Center Line and Width—A Study on River Brahmaputra. *J. Indian Soc. Remote Sens.* **2013**, *42*, 475–482. [CrossRef]
8. Monegaglia, F. Meandering Rivers Morphodynamics—Integrating Nonlinear Modeling and Remote Sensing. 2017, p. 250. Available online: http://qmro.qmul.ac.uk/xmlui/handle/123456789/33927 (accessed on 1 September 2022).
9. Ashworth, P.J.; Best, J.L.; Roden, J.E.; Bristow, C.S.; Klaassen, G.J. Morphological evolution and dynamics of a large, sand braid-bar, Jamuna River, Bangladesh. *Sedimentology* **2000**, *47*, 533–555. [CrossRef]
10. Gilvear, D.; Winterbottom, S.; Sichingabula, H. Character of channel planform change and meander development: Luangwa River, Zambia. *Earth Surf. Process. Landf.* **2000**, *25*, 421–436. [CrossRef]
11. Mosselman, E. Morphological modelling of rivers with erodible banks. *Hydrol. Process.* **1998**, *12*, 1357–1370. [CrossRef]
12. Mosselman, E. A review of mathematical models of river planform changes. *Earth Surf. Process. Landf.* **1995**, *20*, 661–670. [CrossRef]
13. Winterbottom, S.; Gilvear, D. A GIS-based approach to mapping probabilities of river bank erosion: Regulated River Tummel, Scotland. *Regul. Rivers Res. Manag.* **2000**, *16*, 127–140. [CrossRef]

14. Boothroyd, R.; Williams, R.; Barrett, B.; Hoey, T.; Tolentino, P.; Perez, J.; Guardian, E.; David, C.; Yang, X. Detecting and Quantifying Morphological Change in Tropical Rivers Using Google Earth Engine and Image Analysis Techniques. In *River Flow 2020*; CRC Press: Boca Raton, FL, USA, 2020; pp. 1013–1021. [CrossRef]
15. Basnayaka, V.; Samarasinghe, J.T.; Gunathilake, M.B.; Muttil, N.; Hettiarachchi, D.C.; Abeynayaka, A.; Rathnayake, U. Analysis of Meandering River Morphodynamics Using Satellite Remote Sensing Data—An Application in the Lower Deduru Oya (River), Sri Lanka. *Land* **2022**, *11*, 1091. [CrossRef]
16. Hemati, M.; Hasanlou, M.; Mahdianpari, M.; Mohammadimanesh, F. A Systematic Review of Landsat Data for Change Detection Applications: 50 Years of Monitoring the Earth. *Remote Sens.* **2021**, *13*, 2869. [CrossRef]
17. Wray, R.A. Palaeochannels of the Namoi River Floodplain, New South Wales, Australia: The use of multispectral Landsat imagery to highlight a Late Quaternary change in fluvial regime. *Aust. Geogr.* **2009**, *40*, 29–49. [CrossRef]
18. Schwenk, J.; Khandelwal, A.; Fratkin, M.; Kumar, V.; Foufoula-Georgiou, E. High spatiotemporal resolution of river planform dynamics from Landsat: The RivMAP toolbox and results from the Ucayali River. *Earth Space Sci.* **2017**, *4*, 46–75. [CrossRef]
19. Nagel, G.W.; Novo, E.M.L.D.M.; Martins, V.S.; Campos-Silva, J.V.; Barbosa, C.C.F.; Bonnet, M.P. Impacts of meander migration on the Amazon riverine communities using Landsat time series and cloud computing. *Sci. Total Environ.* **2022**, *806*, 150449. [CrossRef]
20. Shelton, S.; Lin, Z. Streamflow Variability in Mahaweli River Basin of Sri Lanka during 1990–2014 and Its Possible Mechanisms. *Water* **2019**, *11*, 2485. [CrossRef]
21. Rubel, F.; Kottek, M. Observed and projected climate shifts 1901-2100 depicted by world maps of the Köppen-Geiger climate classification. *Meteorol. Z.* **2010**, *19*, 135–141. [CrossRef]
22. Withanachchi, S.S.; Köpke, S.; Withanachchi, C.R.; Pathiranage, R.; Ploeger, A. Water Resource Management in Dry Zonal Paddy Cultivation in Mahaweli River Basin, Sri Lanka: An Analysis of Spatial and Temporal Climate Change Impacts and Traditional Knowledge. *Climate* **2014**, *2*, 329–354. [CrossRef]
23. Ranasinghe, P.; Fernando, G.; Dissanayake, C.; Rupasinghe, M. Stream sediment geochemistry of the Upper Mahaweli River Basin of Sri Lanka—Geological and environmental significance. *J. Geochem. Explor.* **2008**, *99*, 1–28. [CrossRef]
24. Dissanayake, C.B.; Weerasooriya, S.V.R. The environmental chemistry of Mahaweli river, Sri Lanka. *Int. J. Environ. Stud.* **1986**, *28*, 207–223. [CrossRef]
25. Hansen, M.C.; Loveland, T.R. A review of large area monitoring of land cover change using Landsat data. *Remote Sens. Environ.* **2012**, *122*, 66–74. [CrossRef]
26. Isikdogan, F.; Bovik, A.; Passalacqua, P. RivaMap: An automated river analysis and mapping engine. *Remote Sens. Environ.* **2017**, *202*, 88–97. [CrossRef]
27. Feyisa, G.L.; Meilby, H.; Fensholt, R.; Proud, S.R. Automated Water Extraction Index: A new technique for surface water mapping using Landsat imagery. *Remote Sens. Environ.* **2014**, *140*, 23–35. [CrossRef]
28. Crist, E.P. A TM Tasseled Cap equivalent transformation for reflectance factor data. *Remote Sens. Environ.* **1985**, *17*, 301–306. [CrossRef]
29. McFeeters, S.K. The use of the Normalized Difference Water Index (NDWI) in the delineation of open water features. *Int. J. Remote Sens.* **1996**, *17*, 1425–1432. [CrossRef]
30. Xu, H. Modification of normalised difference water index (NDWI) to enhance open water features in remotely sensed imagery. *Int. J. Remote Sens.* **2006**, *27*, 3025–3033. [CrossRef]
31. Fisher, A.; Flood, N.; Danaher, T. Comparing Landsat water index methods for automated water classification in eastern Australia. *Remote Sens. Environ.* **2016**, *175*, 167–182. [CrossRef]
32. Danaher, T.; Collett, L. Development, Optimisation and Multi-Temporal Application of a Simple Landsat based Water Index. In Proceedings of the The 13th Australasian Remote Sensing and Photogrammetry Conference, Canberra, Australia, 20–24 November 2006.
33. Raheem, F.S.; Alwan, A.H. Development of a New Water Index for Landsat Operational Land Imager (OLI) Data Using Bayesian Optimization. *J. Adv. Res. Dyn. Control. Syst.* **2018**, *10*, 1–6. Available online: http://earthexplorer.usgs.gov (accessed on 1 September 2022).
34. Zhang, G.; Zheng, G.; Gao, Y.; Xiang, Y.; Lei, Y.; Li, J. Automated Water Classification in the Tibetan Plateau Using Chinese GF-1 WFV Data. *Photogramm. Eng. Remote Sens.* **2017**, *83*, 509–519. [CrossRef]
35. Xia, H.; Zhao, J.; Qin, Y.; Yang, J.; Cui, Y.; Song, H.; Ma, L.; Jin, N.; Meng, Q. Changes in Water Surface Area during 1989–2017 in the Huai River Basin using Landsat Data and Google Earth Engine. *Remote Sens.* **2019**, *11*, 1824. [CrossRef]
36. Zou, Z.; Xiao, X.; Dong, J.; Qin, Y.; Doughty, R.B.; Menarguez, M.A.; Zhang, G.; Wang, J. Divergent trends of open-surface water body area in the contiguous United States from 1984 to 2016. *Proc. Natl. Acad. Sci. USA* **2018**, *115*, 3810–3815. [CrossRef]
37. Zou, Z.; Dong, J.; Menarguez, M.A.; Xiao, X.; Qin, Y.; Doughty, R.B.; Hooker, K.V.; Hambright, K.D. Continued decrease of open surface water body area in Oklahoma during 1984–2015. *Sci. Total Environ.* **2017**, *595*, 451–460. [CrossRef] [PubMed]
38. Chen, B.; Xiao, X.; Li, X.; Pan, L.; Doughty, R.; Ma, J.; Dong, J.; Qin, Y.; Zhao, B.; Wu, Z.; et al. A mangrove forest map of China in 2015: Analysis of time series Landsat 7/8 and Sentinel-1A imagery in Google Earth Engine cloud computing platform. *ISPRS J. Photogramm. Remote Sens.* **2017**, *131*, 104–120. [CrossRef]
39. USGS. Landsat Enhanced Vegetation Index. U.S. Geological Survey. Available online: https://www.usgs.gov/landsat-missions/landsat-enhanced-vegetation-index (accessed on 3 August 2022).
40. Rohatgi, A. Webplotdigitizer: Version 4.5. 2021. Available online: https://automeris.io/WebPlotDigitizer (accessed on 1 September 2022).
41. Furbish, D.J. River-bend curvature and migration: How are they related? *Geology* **1988**, *16*, 752. [CrossRef]